Auto-ranging DSM-ADC and LED Communication for Whole-life Neural Recording Module

Jaeouk Cho[1], Geunchang Seong [1], Hongkyun Kim[1], Dongyeol Seok [1], and Chul Kim[1,2]

[1, a] Department of Bio and Brain Engineering, Korea Advanced Institute of Science and Technology

[2] Department of Electrical Engineering, Korea Advanced Institute of Science and Technology

E-mail : [1]jjo2883@kaist.ac.kr

***Abstract* - This paper focused on establishing a closed-loop stimulation environment capable of accommodating multiple experimental animals. The key requirement for closed-loop stimulation is the ability to measure neural signals within the stimulation environment. To achieve simultaneous measurement of stimulation artifacts in the range of tens of mV and neural signals in the range of hundreds of μV, a recording system with a large dynamic range is essential to prevent saturation caused by the high-intensity stimulation artifacts. Furthermore, to transmit the acquired data externally, down-sampling is essential to reduce power consumption. In this work, delta-sigma (DS) modulation and digital prediction techniques are used to ensure a high dynamic range and prevent saturation in the recording stage. Additionally, to facilitate the simultaneous transmission of data from multiple animals without signal degradation, an internal cascaded integrator-comb (CIC) filter is utilized to encode the down-sampled data. The proposed approach enables the creation of a robust closed-loop stimulation recording system capable of handling multiple subjects while maintaining data integrity. We present 8 channel neural recording chip with a 65-nm CMOS process and the entire chip area is 1 mm^2. Two signals were transmitted and received at a distance of 10 cm with a 1 Mbit data rate without an error.**

***Keywords*—Closed loop neural stimulation, Wireless communication, Decimation filter, Delta sigma ADC**

I. INTRODUCTION

As life expectancy increases, the prevalence of neurodegenerative disorders such as Parkinson's disease and Alzheimer's disease is rapidly rising [1]. Various attempts have been made to treat degenerative neurological disorders through methods including medication and surgery. It has been revealed that neural stimulation is effective in treating these conditions [2]. Currently, deep brain stimulation (DBS) is widely used for alleviating Parkinson's disease and treating other neurological disorders such as Alzheimer's disease, epilepsy, and depression [3].

Neural stimulation methods can be classified into non-invasive and invasive approaches. Invasive methods require surgery for neural stimulation, they offer high specificity,

a. Corresponding author; kimchul@kaist.ac.kr

Manuscript Received May. 31, 2023, Revised Sep. 11, 2023, Accepted Sep. 27, 2023

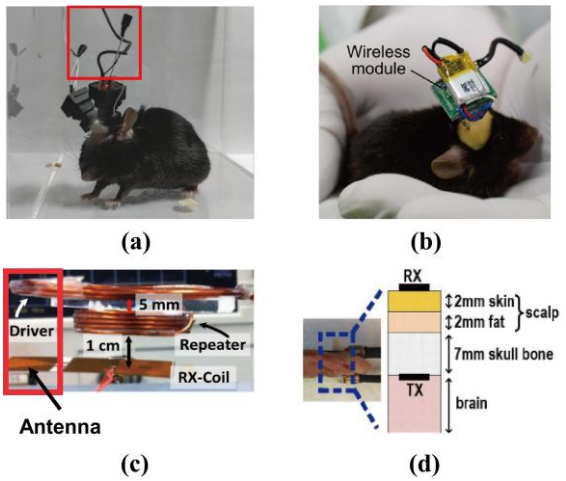

Fig. 1. Diverse data transmission methods for implant neural recording devices. (a) Wired data transmission [4], (b) Bluetooth [5], (c) RF coil [6], and (d) Inductive coupling [7].

allowing precise targeting of the desired regions and thus enhancing therapeutic efficacy [8],[9]. In particular, there has been extensive research on implementing closed-loop stimulation systems tailored to individual patient conditions. However, one of the challenges in closed-loop stimulation is the design of measurement devices that can operate within the stimulating environment. To simultaneously measure neural signals along with stimulation artifact signals, a wide dynamic range neural recording system is required. The most significant issue lies in the use of wired systems for power supply and transmission of measured data. To address these challenges, many researches use battery-powered systems for power supply and wireless data transmission methods for transmitting the measured data.

Various data transmission methods have been extensively researched. Fig. 1. provides an overview of different methods used for external data transmission, including wired systems, Bluetooth, inductive coupling, and radio frequency (RF) methods. Table. 1. presents a comparative analysis of various data transmission methods, discussing their advantages and disadvantages. This analysis aims to provide insights into the strengths and limitations of each method. Bluetooth-based communication requires separate external chips and components, which cannot be directly integrated into the circuit, thereby requiring a larger area. Moreover, Bluetooth uses the 2402MHz~2480MHz frequency band for data transmission, necessitating additional circuitry to generate higher frequencies, adding complexity to the circuitry integrated within the chip. Radio frequency-based

TABLE I. Comparison of Wireless Data Transmission Methods

		Data rate [Mbps]	Power Consumption [mW]	Area [mm²]	Distance [cm]
Bluetooth [5]		0.5	20	120	$< 10^3$
Inductive [7]		200	0.3	100	1.1
RF	[6]	100	5	100	$< 10^3$
	[10]	6.78	10.3	> 30cm Antenna	
μLED based structure		> 50	< 1[11]	< 0.01	< 20

wireless communication utilizes antennas for wireless communication and offers the advantage of longer transmission distances. However, it requires a larger area due to the presence of the antenna and higher power consumption. Additionally, it requires a complex system with separate components to generate high carrier frequencies. Inductive coupling-based wireless communication involves changing the presence or absence of power transmission and modifying the frequency, amplitude, and phase of the transmitted signal to convey data. This method allows simultaneous power transmission and data communication, but the coil size cannot be reduced to ensure power and communication efficiency. Furthermore, as the distance between the coils increases, the data transfer rate decreases rapidly, limiting communication to short distances.

This paper presents a system that can operate in stimulation enabling multiple experimental animals to freely move while allowing neural recording and stimulation. The recording part was designed by targeting ECOG and designed to measure signals in the 0-500 Hz band. Wireless transmission of neural signal data from multiple individuals was also introduced. High dynamic neural recording systems and led-based communication circuits are described in Section II. The simulation and experiment results of the circuit are presented in Section III. Finally, concluded the paper in Section IV.

II. DESIGN METHODOLOGY

A. Neural recording circuit design and implementation

For neural recording to function optimally in electrically stimulated environments, the system necessitates a high dynamic range. Previous research predominantly focused on designing for measuring small neural signals, utilizing signal amplification and analog-to-digital conversion (ADC). However, when stimulation artifacts accompany neural signals, the output signal of the amplification stage becomes saturated due to the presence of large stimulation artifacts. Therefore, in this paper, a direct ADC structure capable of digitizing signals without amplification, along with digital auto-ranging for measuring large input signals, was designed to enable recording neural in stimulated environments [12].

Delta-sigma (DS) ADCs can measure small signals without the need for amplifiers by shaping quantization noise into higher frequencies. The Capacitive DAC (CDAC)

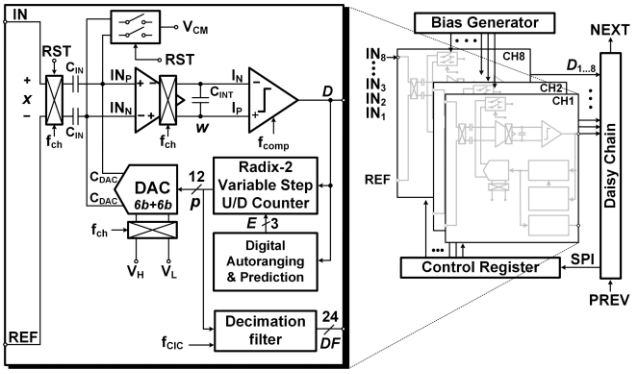

Fig. 2. 8 channel circuit implementation and detailed circuit diagram.

stores the tracked values of previous signals and compares with the next input signal. By continuously measuring the difference between successive signals through the CDAC, this framework allows for more precise signal measurements. The input ADC can be effectively reduced, leading to improved linearity within the system, and facilitating more precise and accurate signal measurements. The output of the comparator determines the update direction of the signal stored in the CDAC. Digital auto-ranging structure determines the update magnitude of the feedback signal based on the previous output values of the comparator. If the update magnitude of the feedback DAC is too large, it becomes challenging to track fine signals, while too small of an update requires a significant amount of time to track large signals. Thus, choosing the update magnitude in the recording system is important. Detailed information on the structure and algorithm associated with digital auto-ranging can be found in [12].

The sampling frequency of the recorded data is increased by oversampling at a rate that is a multiple of the Nyquist sampling rate, referred to as the oversampling rate (OSR), to reduce quantization noise. The oversampled data is not directly transmitted externally to improve efficiency. Instead, the data is down-sampled by dividing the over sampled frequency by the down-sampling rate (D). When down-sampling is performed, high-frequency noise that has been shaped is brought down to lower frequencies, resulting in noise aliasing. Therefore, before down-sampling, it is necessary to utilize a low-pass filter (LPF) to filter out the high-frequency noise. The combination of LPF and down-sampling is referred to as a decimation filter, and one of the famous structures of decimation filter structures is the Cascade Integrator Comb (CIC) filter. The CIC filter consists of integrators, down-sampling, and differentiators, with the number of stages determined by the order of the filter as shown in Fig. 3. (a). The number of stages determines the order of the CIC filter. The advantage of the CIC filter lies in its hardware-friendly implementation, as it does not require multipliers or memory [13]. Thus, we used the CIC filter for the decimation process. Fig. 3. (b) illustrates the simulation results in MATLAB. The figure represents the frequency response of the second-order CIC filter with D set to 64. The frequency response exhibits an LPF characteristic that decreases at a rate of 40 dB/dec [13]. This characteristic enables the reduction of aliasing noise during the down-sampling process.

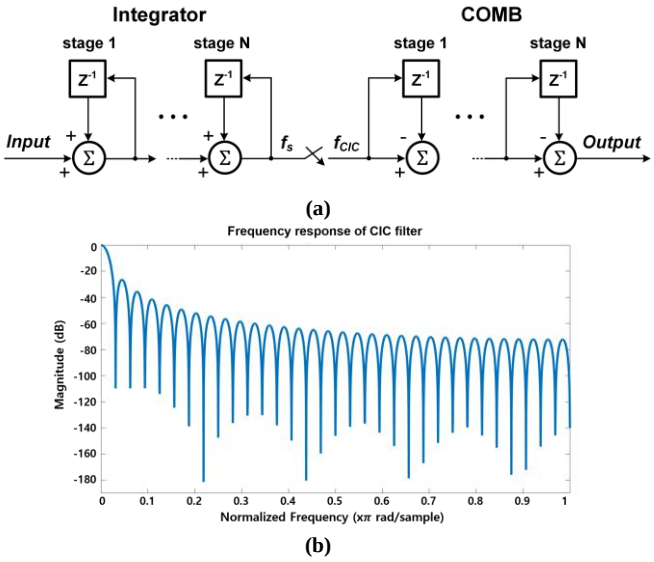

Fig. 3. (a) Structure of an Nth-order CIC Filter. (b) Frequency response of proposed 64 down-sampled 2nd order CIC filter.

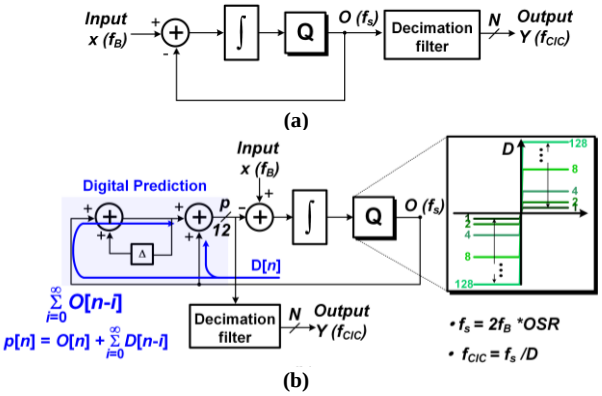

Fig. 4. Decimation filter for down-sampling. (a) Decimation filter in a conventional 1bit DSM ADC and (b) proposed structure.

In conventional DS-ADC, the output of the comparator is used as the input to the decimation filter as shown in Fig. 4. (a). However, in the proposed structure, as depicted in Fig. 4. (b), the weight of the feedback signal is varied due to the digital auto-ranging block. Thus, it's hard to use the comparator as the input of the decimation filter. As the decimation input, the output of the digital integrator is used as the input.

B. LED based wireless communication

If the decimated signals were directly transmitted externally, the data from each animal would be measured simultaneously by photodiodes, resulting in signal distortion. To create a cage where multiple subjects can coexist, it is necessary to enable the communication of multiple data streams simultaneously. The three main methods for achieving simultaneous communication are frequency division multiple access (FDMA), time division multiple access (TDMA), and code division multiple access (CDMA). FDMA increases the complexity of the transmitter (TX) side, while TDMA requires a communication environment

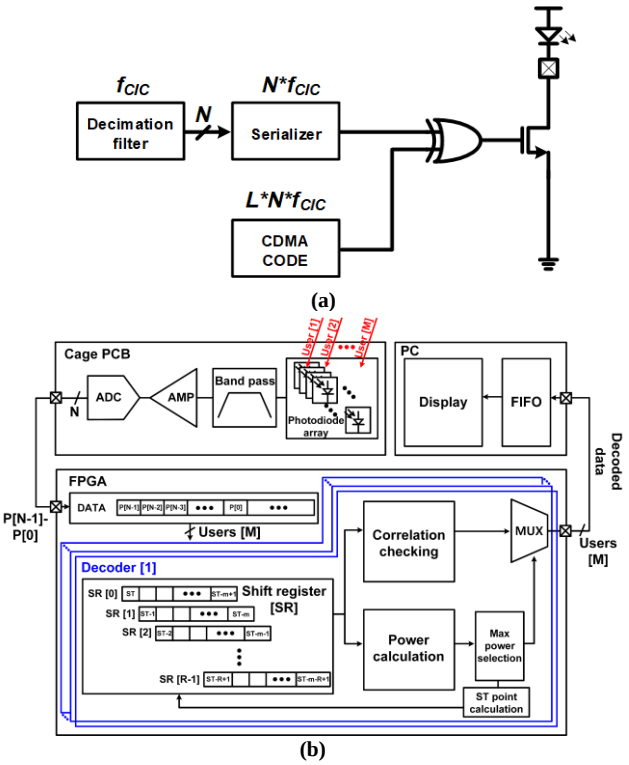

Fig. 5. (a) Circuit structure for encoding. (b) Wireless data receiving structure using LEDs.

between the TX and receiver (RX), making it more complex compared to CDMA. CDMA structure was selected to accommodate the neural signals from multiple animals. CDMA has the advantage of being less affected by noise during the process of spreading the original data by the code length and adding it back, resulting in effective operation regardless of noise interference. Fig. 5. (a) represents N-bit decimated data is serialized, and then encoded using XOR operations with a code of length L. The encoded data is transmitted externally via LEDs. Fig. 5. (b) shows the structure for receiving LED signals. Each subject's data is detected by a photodiode array and transmitted signals undergo bandpass filtering and amplification before being digitized through an ADC. The digitized data is then transferred to a field programmable gate array (FPGA), which is designed to decode each CDMA code. Finally, the decoded data is displayed on a PC for visualization.

In CDMA, if the starting point of the operation deviates from the assigned code, the original signal cannot be decoded. Therefore, in CDMA communication, it is crucial to synchronize the assigned codes with the received signals to determine the starting point for the XOR. When utilizing CDMA in multi-animal communication, several issues need to be solved. The first issue occurs from the fact that each implanted device operates with an independent clock signal. Due to the independent clocks, the correlation between the codes used by different devices becomes non-zero, resulting in mutual interference during decoding. To mitigate this issue, pseudo-random codes with low correlation instead of Walsh codes, which form perfect orthogonal codes even when the codes are not synchronized, were used. The second issue is made by the independent operation of the transmitter

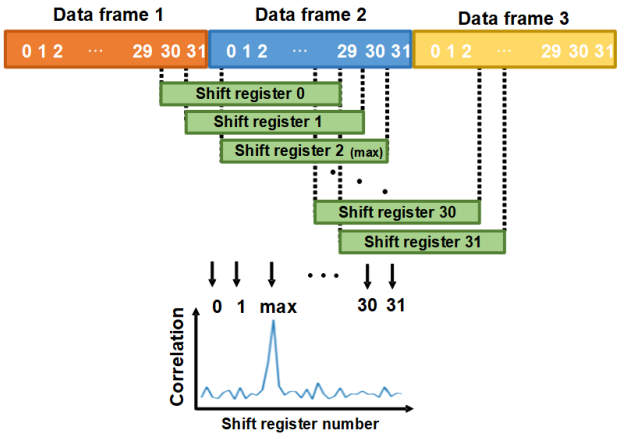

Fig. 6. Encoding starting position decisions using shift resistors.

and receiver. When the receiver samples the signal at the transition points from 1 to 0 or from 0 to 1 in the transmitted data, it cannot determine the data value accurately. Although increasing the resolution of the analog-to-digital converter or raising the sampling rate can reduce the errors introduced by sampling, but it cannot fundamentally solve the problem. Therefore, in this study, the sampling was performed at least twice the communication frequency, and the average value of the obtained signal was used to determine the original signal value even at points of signal variation caused by sampling.

As shown in Fig. 6, if the decoding starts at an incorrect point, the inner product between the received data and the code produces a low result, whereas it reaches its maximum only when the decoding is performed at the desired point. The shift register of the length of the code was implemented in the FPGA, and the data was stored bit by bit as it shifted through each register. The decoding starts at the point where the inner product between the stored data in the register and the assigned code yields the maximum value, allowing the data to be recovered accurately.

III. RESULTS AND DISCUSSIONS

Unfortunately, the chip we designed did not function correctly. The reason for its malfunction was identified as the reversal of the feedback path direction into the integrator from the DAC, causing the entire system to operate with positive feedback, rendering the ADC inoperative. Subsequently, the provided data is based on simulation results obtained after post-extraction analysis. The provided Fig. 7. (a) presents the results of the Cadence simulation, illustrating the reconstructed output values of the designed ADC with and without the use of the auto-ranging block. The simulation was conducted with the simultaneous input of a 50Hz pulse signal with an amplitude of 100mV, and a 500Hz sine signal with an amplitude of 1mV. The figure demonstrates that when the auto-ranging block is not employed, significant delays are observed in tracking the larger pulse signal. Conversely, when the auto-ranging block is utilized, it is evident that the ADC rapidly follows the larger signal by adjusting its step size. Fig. 7. (b) shows the plot of the output signal before and after the CIC filter and subsequently applying a 500Hz brick wall filter using MATLAB.

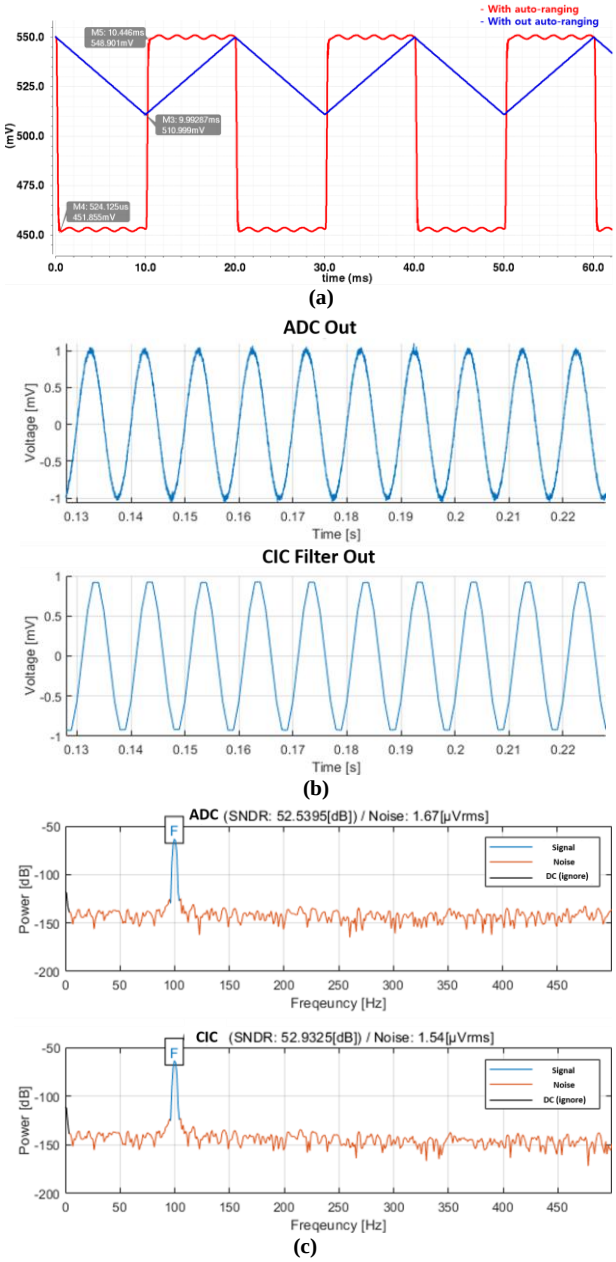

Fig. 7. (a) Reconstructed ADC output with or without auto ranging block (b) Input and output of CIC filter. (c) SNDR value of Input and output of CIC filter.

The input signal for this plot is the 100Hz sine signal with an amplitude of 1 mV. As depicted in Fig. 7. (c), the Signal-to-Noise and Distortion Ratio (SNDR) of the signal shows minimal variation before and after passing through the CIC filter. Inside a CIC filter, adders and subtractors are used, so it's important to consider bit overflow. To prevent overflow, the number of bits used within the CIC filter should be determined as M + K * log2(N) [14]. Here, M represents the input bits, K represents the filter order, and N represents the down-sampling rate. In this work, a 12-bit input is provided to the CIC filter, and the CIC filter has a 2nd-order with a down-sampling rate of 64. Therefore, the final number of bits used in the CIC filter is set to 24 bits. The total area of the CIC filter is 2850 um^2. The power consumption of the 1CH CIC filter was 55nW.

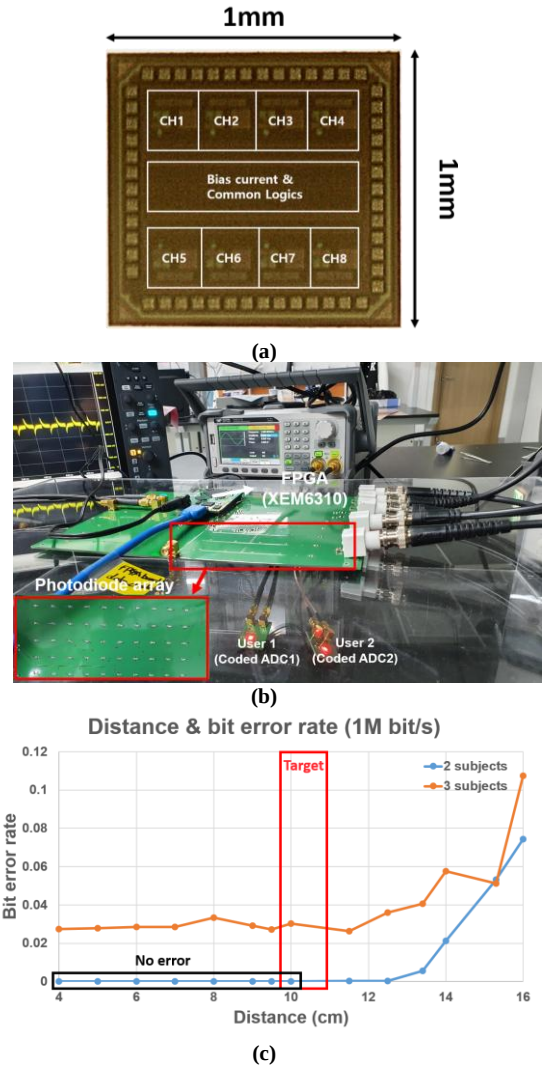

Fig. 8. (a) Fabricated chip diagram. Wireless communication experiment using LEDs. (b) Measurement setup for transmitting the 2 encoded ADC data using LEDs and then receiving it through a photodiode array for decoding. (c) Bit error rate according to the distance of 1Mbit/s data rate signal.

Fig. 8. (a) represents the Fabricated chip. The entire chip area is 1mm*1mm in size and consists of a total of 8 channels. The performance evaluation using PEX simulation is shown in TABLE II. Fig. 8. (b) illustrates the wireless data experimental setup replicating the diagram shown in Fig. 5. (c) User 1 and User 2 simulate the roles of transmitting the coded ADC results. The environment is designed to transmit data in the form of 1s and 0s using a signal generator to drive the LEDs, and the transmitted data is received using a photodiode array located beneath a PCB. The data measured using the photodiode array undergoes bandpass filtering and amplification before being digitized using a commercial ADC. The digitized data is then processed through a FPGA and the results are displayed on a computer screen. Fig. 8. (c) represents the data transmission error rate as a function of distance. When the experiment was conducted using two LEDs, there were no errors observed for distances up to the target value of 10cm. However, beyond a 10cm distance, errors began to occur and the error rate increased. When three LEDs were used for communication, it was found that

TABLE II. Comparison Table

	[15]	[16]	[17]	This work
Power/CH (μW)	7.3	6	6.8	1.6
Supply (V)	1.2	0.8	1.2	1
Operation frequency (Hz)	400k	320k	1.6M	64k
Noise density ($nV/\sqrt{Hz}$)	127	379	82	44.7
ENOB (bits)	14	8.8	11.3	10.6
Process (nm)	40	22	180	z65

even at a distance of 4 cm, the bit error rate exceeded 0.001. This was attributed to the usage of pseudo-random codes that do not have orthogonality, causing increased interference between signals during decoding as the number of objects transmitting signals increased.

IV. CONCLUSION

In this study, we developed a measurement system capable of operating in a closed-loop stimulation system and designed a wireless data transmission system using LEDs and CDMA technology to transmit data from multiple animal's neural data wirelessly. To measure neural signals in a stimulation environment, we employed a delta-sigma structure and a variable comparator. To widen the dynamic range, we added an integrator in the feedback path to track the input signal and process only its changes, resulting in a measurement-capable structure. In the wireless data transmission research, we addressed the limitations of existing wireless communication methods, such as high complexity, large area requirements, and difficulties in transmitting data from multiple animals. To overcome these challenges, we utilized low-complexity LEDs and photodiode arrays for wireless communication. By simultaneously transmitting data using two LEDs, we successfully developed a system that achieved error-free communication up to 10 cm at a data rate of 1M per second. The experimental findings indicate that the wireless data communication system using LEDs encounters challenges related to distance, data rate, and interference between signals. The non-ideal characteristics of the LEDs and the use of pseudo-random codes contribute to the occurrence of errors and increased error rates as the distance and data rate increase. When utilizing CDMA in multi-animal communication, several issues need to be solved.

ACKNOWLEDGMENT

This work was supported by the National Research Foundation of Korea (NRF) grant funded by the Korea government (MSIT) (No.2020R1C1C1009878) and has been supported by the ETRI (Electronics and Telecommunications Research Institute)'s internal funds. [21YR2500, Development of Digital Biopsy Core Technology for high-precision Diagnosis and Therapy of Senile Disease]. The chip fabrication was supported by the IC Design Education Center (IDEC), Korea.

REFERENCES

[1] Reitz, Christiane, Carol Brayne, and Richard Mayeux, Epidemiology of Alzheimer disease, Nature Reviews Neurology, 2011.
[2] Benabid, Alim-Louis, et al., Combined (thalamotomy and stimulation) stereotactic surgery of the VIM thalamic nucleus for bilateral Parkinson disease, Stereotactic and functional neurosurgery ,1987.
[3] Chang, Chun-Hung, Hsien-Yuan Lane, and Chieh-Hsin Lin., Brain stimulation in Alzheimer's disease, Frontiers in psychiatry 9, 2018.

[4] de Groot, Andres, et al. "NINscope, a versatile miniscope for multi-region circuit investigations.", *Elife, Eng.*, 2020
[5] Idogawa, Shinnosuke, et al. "A lightweight, wireless Bluetooth-low-energy neuronal recording system for mice.“, Sensors and Actuators B: Chemical . Eng., 2021
[6] Mirbozorgi, S. Abdollah, et al. "A single-chip full-duplex high speed transceiver for multi-site stimulating and recording neural implants." IEEE transactions on biomedical circuits and systems . Eng., 2016
[7] W. Li, Y. Duan and J. M. Rabaey, "A 200Mb/s inductively coupled wireless transcranial transceiver achieving 5e-11 BER and 1.5pJ/b transmit energy efficiency," IEEE International Solid - State Circuits Conference - (ISSCC), Eng., 2018
[8] Chen, K.-H. S. and Chen, R., Invasive and noninvasive brain stimulation in Parkinson’s disease: clinical effects and future perspectives, Clinical Pharmacology & Therapeutics 106, 2019.
[9] Theodore, William H., and Robert S. Fisher., Brain stimulation for epilepsy, The Lancet Neurology 3.2, 2004.
[10] Jia, Yaoyao, et al. "A trimodal wireless implantable neural interface system-on-chip." IEEE Transactions on Biomedical Circuits and Systems , Eng, 2020
[11] J. J. D. McKendry et al., "Visible-Light Communications Using a CMOS-Controlled Micro-Light- Emitting-Diode Array," in Journal of Lightwave Technology, Eng, 2012
[12] C. Kim, S. Joshi, H. Courellis, J. Wang, C. Miller and G. Cauwenberghs, "Sub- µW Vrms-Noise Sub- µW /Channel ADC-Direct Neural Recording With 200-mV/ms Transient Recovery Through Predictive Digital Autoranging," in IEEE Journal of Solid-State Circuits, vol. 53, no. 11, pp. 3101-3110, 2018
[13] Hogenauer, Eugene. "An economical class of digital filters for decimation and interpolation." IEEE transactions on acoustics, speech, and signal processing 29.2, 1981
[14] Schreier, Richard, and Gabor C. Temes. Understanding delta-sigma data converters. Vol. 74. Piscataway, NJ: IEEE press, 2005.
[15] H. Chandrakumar and D. Markovic, “A 15.2-ENOB continuous-time ΔΣ ADC for a 200mVpp-linear-input-range neural recording front-end,” in *IEEE ISSCC Dig. Tech. Papers*, Feb. 2018, pp. 232–234.
[16] Yang, Xiaolin, et al. "An AC-Coupled 1st-Order Δ-ΔΣ Readout IC for Area-Efficient Neural Signal Acquisition." IEEE Journal of Solid-State Circuits 58.4 (2023):
[17] Oh, Sungjin, et al. "Power-Efficient LFP-Adaptive Dynamic Zoom-and-Track Incremental ΔΣ Front-End for Dual-Band Subcortical Recordings." IEEE Transactions on Biomedical Circuits and Systems (2023).

Jaeouk Cho (Student Member, IEEE) received the B.S. degree in biomedical engineering from Hanyang University, Seoul, Korea, in 2019, and the M.S degree in bio and brain engineering from Korea Advanced Institute of Science and Technology (KAIST), Daejeon, South Korea in 2021. Currently, he is working toward Ph.D. degree in bio and brain engineering at KAIST, Daejeon, Korea. His research interests include Neural recording IC and implantable biomedical devices.

Geunchang Seong (Student Member, IEEE) received the B.S. and M.S. degree in bio and brain engineering from Korea Advanced Institute of Science and Technology (KAIST), Daejeon, Republic of Korea, in 2020 and 2022. He is currently pursuing the Ph.D. degree in bio and brain engineering from KAIST. His research interests include bio-signal processing, integrated circuit (IC) chip design for biomedical healthcare system.

Hongkyun Kim (Student Member, IEEE) received the B.S. degree in electrical engineering from Kyunghee University, Suwon, Korea, in 2016, and the M.S. degree from the Graduate School for Green Transportation Engineering, Korea Advanced Institute of Science and Technology (KAIST), Daejeon, Korea, in 2018. Currently, he is working toward Ph.D. degree in bio and brain engineering at KAIST, Daejeon, Korea. His research interests include wireless power transfer system and power management ICs.

Dongyeol Seok received the B.S. degree in bio and brain engineering (major) and in science and technology policy (minor) from Korea Advanced Institute of Science and Technology (KAIST), Daejeon, Republic of Korea, in 2020. He is currently pursuing the M.S. degree in bio and brain engineering, KAIST. His research interests include EEG analog front-end, development of motion artifact-free EEG system, and integrated circuit (IC) chip design for biomedical healthcare system.

Chul Kim (Senior Member, IEEE) is an assistant professor in the Department of Bio and Brain Engineering and the Program of Brain and Cognitive Engineering at Korea Advanced Institute of Science and Technology (KAIST), Daejeon, South Korea. He received the Ph.D. degree in 2017 from bioengineering, UC San Diego, La Jolla, CA, USA, where he was a postdoctoral fellow from 2017 to 2019. From 2009 to 2012, he was with SK HYNIX, Icheon, South Korea, where he designed power management circuitry for dynamic random-access memory. His current research interests include design of energy-efficient integrated circuits and systems for fully wireless brain-machine interfaces and unobtrusive wearable sensors.